THE ASTROPHYSICAL JOURNAL, 519:222–235, 1999 July 1
© 1999. The American Astronomical Society. All rights reserved. Printed in U.S.A.

# THE GALACTIC EVOLUTION OF Si, Ti, AND O ISOTOPIC RATIOS

CONEL M. O'D. ALEXANDER AND LARRY R. NITTLER
Department of Terrestrial Magnetism, Carnegie Institution of Washington, 5241 Broad Branch Road NW, Washington, DC 20015
*Received 1998 June 16; accepted 1999 February 2*

## ABSTRACT

Most meteoritic presolar grains of SiC and $Al_2O_3$ condensed around red giant and asymptotic giant branch (AGB) stars prior to the formation of the solar system. Here we use new and previously published isotopic data of presolar SiC and $Al_2O_3$ grains to constrain the Galactic chemical evolution (GCE) of Si, Ti, and O isotopic ratios. The $^{12}C/^{13}C$ ratios of the SiC grains limit the amount of He-shell material mixed to the surface of the parent AGB stars during third dredge-up to a few percent. Thus, the linear correlations observed between the SiC Si and Ti isotopic ratios probably reflect the average GCE trends of these elements. Moreover, the close proximity of these trends to the solar isotopic composition indicates that the latter cannot be very unusual for these elements. A $\chi^2$ fit to the SiC isotopic data has allowed us to accurately estimate the relative GCE paths for the Si and Ti isotopes. The fit estimates the nucleosynthetic components of the grains' compositions, the metallicities of their parent stars, and the mean GCE paths of the isotopes. For most of the isotopes, our results agree remarkably well with the GCE calculations of Timmes, Woosley, & Weaver and Timmes & Clayton after they are corrected to pass through solar. However, the abundances of both $^{30}Si$ and $^{47}Ti$ in the fit increase significantly more slowly with metallicity, relative to the other isotopes, than predicted by the corrected GCE model. Conversely, $^{49}Ti$ increases more rapidly in the fit than predicted. These discrepancies probably reflect errors in the supernova models used to calculate the GCE paths. Our fit also suggests that the typical ISM at solar metallicity is enriched in $^{29}Si$ and $^{30}Si$ (by $\sim 8\%$ and $\sim 5\%$, respectively) relative to solar. The GCE of the O isotopes cannot yet be so well constrained, but the $Al_2O_3$ data are most consistent with a GCE path that passes close to solar rather than one that is $^{18}O$ depleted as suggested by measurements of molecular clouds. The inferred depletion of $^{29}Si$ and $^{30}Si$ in the Sun could be explained by the addition or removal of a small amount of supernova material. However, we can probably rule out a supernova explanation for the apparent enrichment of solar O relative to young stars and the local ISM and $^{18}O$ relative to molecular clouds.

*Subject headings:* dust, extinction — Galaxy: evolution — ISM: abundances — nuclear reactions, nucleosynthesis, abundances — stars: AGB and post-AGB

## 1. INTRODUCTION

Five types of presolar, circumstellar grains have now been isolated from meteorites (Anders & Zinner 1993; Ott 1993; Zinner 1997). The majority of two presolar grain types, SiC and $Al_2O_3$, appear to have condensed in the massive stellar winds of red giant branch (RGB) and asymptotic giant branch (AGB) stars (e.g., Zinner, Tang, & Anders 1989; Hoppe et al. 1994; Huss et al. 1994; Nittler et al. 1997). Both astronomical observations (Smith & Lambert 1990) and theoretical modeling (Iben 1991) of these stars show that a series of dredge-up episodes mix freshly synthesized material from their interiors into their envelopes. The first and second dredge-ups, which occur at the start of the RGB and AGB, respectively, bring CNO-cycle products to the surface. As a result, RGB and early-AGB stars typically exhibit large enrichments in $^{13}C$, $^{14}N$, and $^{17}O$. There is spectroscopic evidence for the condensation of $Al_2O_3$ around giant stars during these stages (Sloan, Levan, & Little-Marenin 1996; Begemann et al. 1997), and most presolar $Al_2O_3$ grains have large $^{17}O$ enrichments, as would be expected if they came from these stars.

Farther along the AGB, during the thermally pulsing (TP-AGB) phase, the so-called third dredge-up episodically brings to the surface the products of He burning and the *s*-process from the He shell. The surface expressions of the third dredge-up include progressive enrichments in $^{12}C$, the principle product of He burning, and elements such as Ba, which are produced by the *s*-process. So much $^{12}C$ is brought to the surface in a $\sim 1.5$–$5\ M_\odot$ star that ultimately the C/O ratio in the envelope exceeds one, creating a carbon star (C star). That SiC condenses around C stars has been recognized for some time (Treffers & Cohen 1974; Merrill & Stein 1976a, 1976b; Cohen 1984) and the distribution of $^{12}C/^{13}C$ ratios in presolar SiC grains is very similar to that of C stars (Smith & Lambert 1990).

Most RGB and AGB stars have initial masses of 1–5 $M_\odot$ and lifetimes of approximately 15–0.7 Gyr, respectively (Mathews, Bazan, & Cowan 1992). The chemical composition of the Galaxy has evolved with time so that given this range of lifetimes, the initial compositions of the RGB and AGB stars that seeded the presolar molecular cloud are expected to reflect this Galactic chemical evolution (GCE). The isotopic compositions of the elements Si, Ti, and O in SiC and $Al_2O_3$ presolar grains, which can be measured with high precision, can only be explained by a combination of nucleosynthesis in the grains' parent stars and GCE (Alexander 1993; Gallino et al. 1994; Hoppe et al. 1994; Nittler et al. 1997). The nucleosynthesis occurring in RGB and AGB stars is better understood than the GCE of these elements. If the nucleosynthetic component can be subtracted from the grains' isotopic compositions, the inferred GCE component would provide stringent tests of GCE models and the supernova models that inform them. This isotopic data would complement astronomical observations

of the elemental abundance variations as a function of metallicity in stars (Gratton & Sneden 1988, 1991; Magain 1989; Edvardsson et al. 1993).

Here we use new and previously published Si, Ti, and O isotopic compositions of presolar SiC and $Al_2O_3$ grains to: (1) examine how representative of the mean GCE the solar isotopic compositions of these three elements are, (2) estimate the fractions of freshly synthesized material that had been added to the envelopes of the parent stars at the times the grains formed, and (3) identify errors in current GCE models for the isotopes of these elements.

## 2. BACKGROUND

Galactic chemical evolution, the buildup of elements heavier than H and He in the Galaxy, is driven largely by the return of freshly synthesized material from supernovae, particularly Type II supernovae. Table 1 lists the major nucleosynthetic reaction mechanisms and stellar sources of the isotopes of the three elements this paper is concerned with. Modelers of nucleosynthesis and GCE often distinguish between primary isotopes, those that ultimately are made from the initial H and He in a star, and secondary isotopes whose synthesis requires heavier seed nuclei formed in a previous generation of stars. Of the three elements considered here, $^{16}$O, $^{28}$Si, and $^{48}$Ti are all primary isotopes. The remaining isotopes are generally considered as secondary. Because secondary isotope synthesis requires preexisting nuclei, their buildup in the Galaxy is initially slower than the primary isotopes, but with time the ratios of secondary to primary isotopes in the Galaxy gradually increase. Consequently, if the solar composition is typical for its age and position in the Galaxy, presolar grains from stars that had lower than solar metallicities should, on average, have lower secondary to primary isotope ratios than solar, and those from higher metallicity stars should have higher ratios. A simplified treatment of GCE suggests that the secondary to primary ratios should increase approximately linearly with metallicity (Clayton 1988). However, GCE is not a uniform, monotonic process throughout the Galaxy. For instance, on large scales the higher densities of stars and gas toward the Galactic center result in more rapid GCE than at greater Galactocentric distances, while on local scales there can be self-enrichment of star-forming regions when massive stars evolve and die before star formation has ceased. Hence, stars of similar metallicity may not only have a range of ages but their isotope ratios will vary depending on the particular nucleosynthetic histories of the materials they formed from. Bearing this in mind, we will assume here that isotopic ratios evolve smoothly in the interstellar medium (ISM), with well-defined average trends relating the isotopic compositions of new stars to their metallicities.

Shown in Figure 1 are the Si isotopic ratios of the so-called mainstream SiC grains, the most populous SiC group, expressed as $\delta$ values—the permil (‰) deviations from the solar ratios. In this figure, the grains plot about a

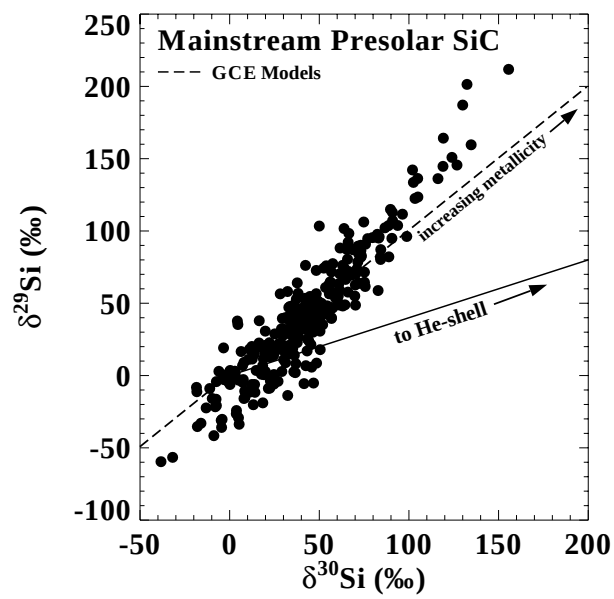


FIG. 1.—Si isotopic compositions of 300 mainstream presolar SiC grains from the Murchison meteorite (Alexander 1993; Hoppe et al. 1994, 1996; this work). Isotopic ratios are expressed as $\delta$ values: $\delta^i\mathrm{Si} = [(^i\mathrm{Si}/^{28}\mathrm{Si})/(^i\mathrm{Si}/^{28}\mathrm{Si})_\odot - 1]1000$. The SiC grains probably formed around C-rich AGB stars that had experienced dredge-up of He-shell material into their envelopes. The slope of the mainstream trend, $\sim 1.3$, is steeper than the slope of $\sim 0.4$ predicted for mixing between a single initial envelope composition and the He shell (Gallino et al. 1994). The slope of the trend is better explained if the grains' parent stars had a range of initial envelope compositions, reflecting Galactic chemical evolution (GCE), that have only been slightly modified by the addition of He-shell material. However, the mainstream trend is also steeper than models of GCE of the Si isotopes, for example, the model of TC96 predicts a slope of about 1 (*dashed line*).

TABLE 1

MAJOR NUCLEOSYNTHETIC REACTION MECHANISMS AND STELLAR SOURCES OF ISOTOPES OF O, Si, AND Ti[a]

| Isotope | Nucleosynthesis Process | Stellar Site |
|---|---|---|
| $^{16}$O ..... | He burning | Type II supernova (SN) |
| $^{17}$O ..... | H burning | Type II SN, AGB |
| $^{18}$O ..... | He burning | Type II SN |
| $^{28}$Si ..... | Explosive and hydrostatic O burning | Type II SN |
| $^{29}$Si ..... | Explosive and hydrostatic Ne burning | Type II SN |
| $^{30}$Si ..... | Explosive and hydrostatic Ne burning | Type II SN |
| $^{46}$Ti..... | Explosive O burning, Ia det.[b] | Type II, Ia SN |
| $^{47}$Ti..... | Explosive O and Si burning, Ia det. | Type II, Ia SN |
| $^{48}$Ti..... | Explosive Si burning, Ia det. | Type II, Ia SN |
| $^{49}$Ti..... | Explosive Si burning, He burning | Type II SN |
| $^{50}$Ti..... | Nuclear statistical equilibrium | Type Ia SN |

[a] After Woosley & Weaver 1995.
[b] Sub-Chandrasekhar detonation Ia (Woosley & Weaver 1994).

line that passes close to the solar composition of $\delta^{29,30}\mathrm{Si} = 0$ and has a slope of about 1.3. Most GCE models of the Si isotopes (Clayton 1988; Gallino et al. 1994; Timmes & Clayton 1996) predict a slope of $\sim 1$ and, because supernova calculations indicate that $^{29}$Si and $^{30}$Si are secondary (Woosley & Weaver 1995), that $\delta^{29}$Si and $\delta^{30}$Si should increase with time and metallicity. It is possible that the GCE models are correct and the steeper slope of the grain data with respect to the models is the result of processes in the parent stars. For instance, Timmes & Clayton (1996) suggested that proportionally more He-shell material may be added to the envelopes of lower metallicity stars (those with near or subsolar $\delta^{29}$Si and $\delta^{30}$Si values), explaining both the steeper slope and the nonsolar intercept of the mainstream grains. This suggestion requires that a relatively high fraction of He-shell material be mixed into the envelopes of lower metallicity stars. Alternatively, Clayton & Timmes (1997) showed that if the Sun has a Si isotopic composition considerably different from the typical interstellar medium, the GCE line will have a slope of $\sim 1.3$ when normalized to the solar abundances. However, in this case the line is displaced some considerable distance, several hundred permil (tens%), from solar, and the mainstream grains therefore require a very large He-shell component to move them from this GCE line to their position in Figure 1. If correct, this would also imply that the proximity of the mainstream trend to solar is a coincidence. On the other hand, the dredge-up of newly synthesized material may have only a minor influence on the Si isotopes of the grains, in which case the difference in slope reflects shortcomings in the GCE models.

Approximately 120 presolar $Al_2O_3$ grains have been found so far (Huss et al. 1994; Nittler et al. 1994; Strebel, Hoppe, & Eberhardt 1997; Nittler et al. 1997; Nittler 1997; Choi et al. 1998). Most of them have large $^{17}$O excesses and modest $^{18}$O depletions (Fig. 2), indicative of partial CNO-cycle burning. These compositions are similar to the observed compositions of RGB and AGB stars (Smith & Lambert 1990). The $^{16}\mathrm{O}/^{17}\mathrm{O}$ ratio of a giant star's envelope depends strongly on stellar mass, which determines both the depth of convective mixing during the first and second dredge-up episodes and the temperature of CNO-cycle burning (Boothroyd, Sackmann, & Wasserburg 1994; El Eid 1994). The $^{16}\mathrm{O}/^{18}\mathrm{O}$ ratio, on the other hand, is much less affected by the dredge-up episodes, so that the $^{16}\mathrm{O}/^{18}\mathrm{O}$ ratio of a presolar grain should more closely reflect the initial composition of its parent star. The spread in presolar $Al_2O_3$ $^{16}\mathrm{O}/^{18}\mathrm{O}$ ratios therefore likely reflects GCE, and, because $^{18}$O is a secondary isotope, the higher than solar ratios of most grains indicate that the parent stars had metallicities lower than solar.

However, one class of grains (group 2, not shown in Fig. 2) has large $^{18}$O depletions, relative to solar, which are not thought to reflect GCE, but instead are possibly the result of an extra mixing process, sometimes termed cool-bottom processing (CBP), that has been proposed to occur in some AGB stars (Wasserburg, Boothroyd, & Sackmann 1995a). Cool-bottom processing likely also occurs on the RGB but does not significantly affect the O isotopes during this phase (Boothroyd & Sackmann 1999). Models predict that the short-lived isotope $^{26}$Al is dredged up into the envelopes of AGB stars, but not RGB stars (Gallino et al. 1994). Many, but not all, $Al_2O_3$ grains show evidence of having contained $^{26}$Al when they formed. Those grains without evidence for

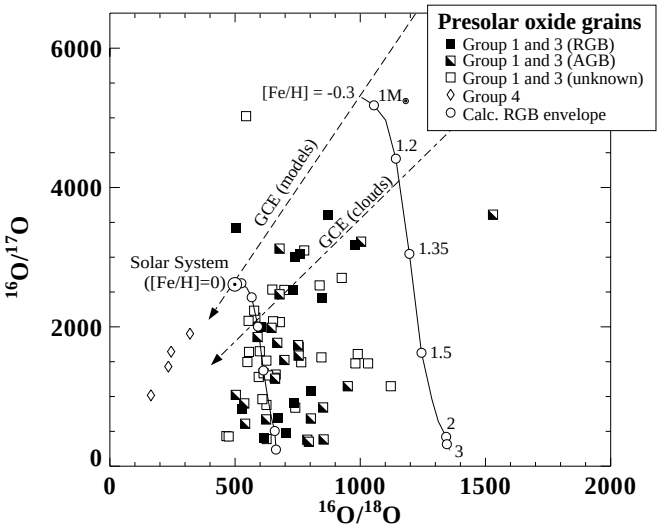


FIG. 2.—Oxygen isotopic compositions of most presolar $Al_2O_3$ grains belonging to groups 1, 3, and 4 (Nittler et al. 1997). Many, but not all, of the grains also contain evidence for having contained $^{26}$Al when they formed. The grains probably originated in RGB and AGB stars. Also shown are the GCE path predicted by the models of Timmes et al. (1995) and Prantzos, Aubert, & Audouze (1996), the GCE path suggested by measurements of the O isotopic compositions of molecular clouds (Penzias 1981b; Wilson & Rood 1994), and the RGB envelope compositions predicted for stars of 1–3 $M_\odot$ and two different metallicities (Boothroyd & Sackmann 1999). Where possible, the group 1 and 3 grains have been divided into those from AGB stars and those from RGB stars, depending on whether or not they show evidence for $^{26}$Al. As can be seen, the stellar evolution up to the beginning of the AGB is not expected to modify the envelope $^{16}\mathrm{O}/^{18}\mathrm{O}$ ratios by more than about 30% from their initial values. Note that the $^{16}\mathrm{O}/^{18}\mathrm{O}$ ratios of some of the grains could have been affected by moderate cool-bottom processing (believed to be the origin of the large $^{18}$O depletions observed in the unshown group 2 oxide grains (Wasserburg et al. 1995b). However, the range in $^{16}\mathrm{O}/^{18}\mathrm{O}$ ratios in the grains without evidence for $^{26}$Al (and hence from RGB stars) demonstrates the grains have come from stars with a range of initial metallicities. Since many of the RGB grains lie above the molecular cloud GCE line, the theoretical line may be more realistic (see § 5).

$^{26}$Al probably came from RGB stars, and, therefore, their isotopic compositions would not have been affected by CBP. It cannot be excluded that the isotopic compositions of some of the AGB grains in Figure 2, especially those grains that appear to have come from $\lesssim 1.6\ M_\odot$ stars, have been influenced by CBP. Nevertheless, the range of compositions of $Al_2O_3$ grains from RGB stars and greater than 1.6 $M_\odot$ AGB stars requires that the parent stars had a range of metallicities.

The GCE lines for the Si and O isotopic ratios shown in Figures 1 and 2 are based on the calculations of Timmes, Woosley, & Weaver (1995, hereafter TWW95) and Timmes & Clayton (1996, hereafter TC96). TWW95 used a standard GCE model to calculate the evolution of all the isotopes of the elements from H to Zn. Their model reproduces the solar abundances to within a factor of 2 for most isotopes at the time the solar system formed. However, even a factor of 2 is too large for direct comparison with the high-precision grain data. TC96 extended the TWW95 model to examine in detail the GCE of Si isotopes, including yields from AGB stars (which were not included in the original calculation of TWW95). Furthermore, they argued that in order to consistently compare GCE models with the grain data, the calculated abundance evolution trends should be first normalized to the calculated composition at the time of

solar system formation. This normalization reduces the influence of uncertainties in the many parameters that go into the models. It also better reproduces the elemental compositions measured in disk stars as a function of metallicity. Of course, the validity of this normalization rests on the assumption that the solar composition is representative of GCE at the time and place the Sun formed. This assumption will be examined in more detail in succeeding sections. Throughout this paper, we will take the TWW95 and TC96 calculations, normalized according to the suggestion of TC96, to be representative of current GCE models. Other GCE models using standard assumptions and nucleosynthetic yields would give the same results.

Despite potential errors in GCE models and remaining uncertainties in the interpretation of the grain data, attempts have been made to infer the metallicity distributions of the stars that produced the grains (Alexander 1997; Nittler et al. 1997, and Fig. 3). These analyses have produced two paradoxical results. First, based on both the Si and Ti isotopic compositions, the majority of the SiC grains apparently came from stars with higher than solar metallicity, despite the fact that the stars must have formed hundreds of millions to billions of years before the solar system formed. Second, the $Al_2O_3$ metallicity distribution differs from that of the SiC; the distribution is wider and extends to considerably lower metallicities. Moreover, the average metallicity of the oxide grain parent distribution is apparently lower than solar, in contrast to that of the SiC. Yet all AGB stars, even those that produce SiC during their final carbon star phase, pass through an oxygen-rich dust producing episode. The interpretation of the presolar $Al_2O_3$ metallicity distribution is complicated by the fact that the mapping technique that was used to find most of the oxide grains is biased against finding presolar $Al_2O_3$ grains with $^{16}O/^{18}O$ ratios within about 10% of the solar value. Grains with compositions in this range are estimated to make up 25%–50% of presolar $Al_2O_3$ grains and would have come from stars with supersolar metallicities. Estimates (based on randomly assigning $^{16}O/^{18}O$ ratios close to solar to the missing grains) for the metallicities of these grains are indicated in Figure 3 by the light and medium gray histograms, corresponding to 50% or 25% of the grains being missed, respectively. Inclusion of these missing grains reduces the difference in the average metallicities inferred from the SiC and $Al_2O_3$ data. However, the distribution for SiC is still much narrower than that for $Al_2O_3$ and still lacks a significant population of subsolar-metallicity stars.

One qualitative explanation for a difference in the metallicity distributions of the sources of the SiC and $Al_2O_3$ grains is that this reflects differences in the mass distributions of the RGB and AGB stars that produced them—proportionately more $Al_2O_3$ grains may come from low-mass ($<1.5\ M_\odot$), longer lived, lower metallicity stars that did not become carbon stars (Alexander 1997). The higher than solar metallicity of most of the SiC-producing stars has been explained by appealing to an overall outward diffusion of stars from the metal-rich inner regions of the Galaxy (Clayton 1997), but this model does not address the $Al_2O_3$ data. However, it has yet to be firmly established that the differences in the inferred metallicity distributions are not, in fact, an artifact of the stellar evolution and GCE models that went into their determination. Also, the inferred higher than solar metallicities of the SiC sources could imply that the Si isotopic composition of the Sun is atypical, rather than being due to stellar dynamics in the Galaxy.

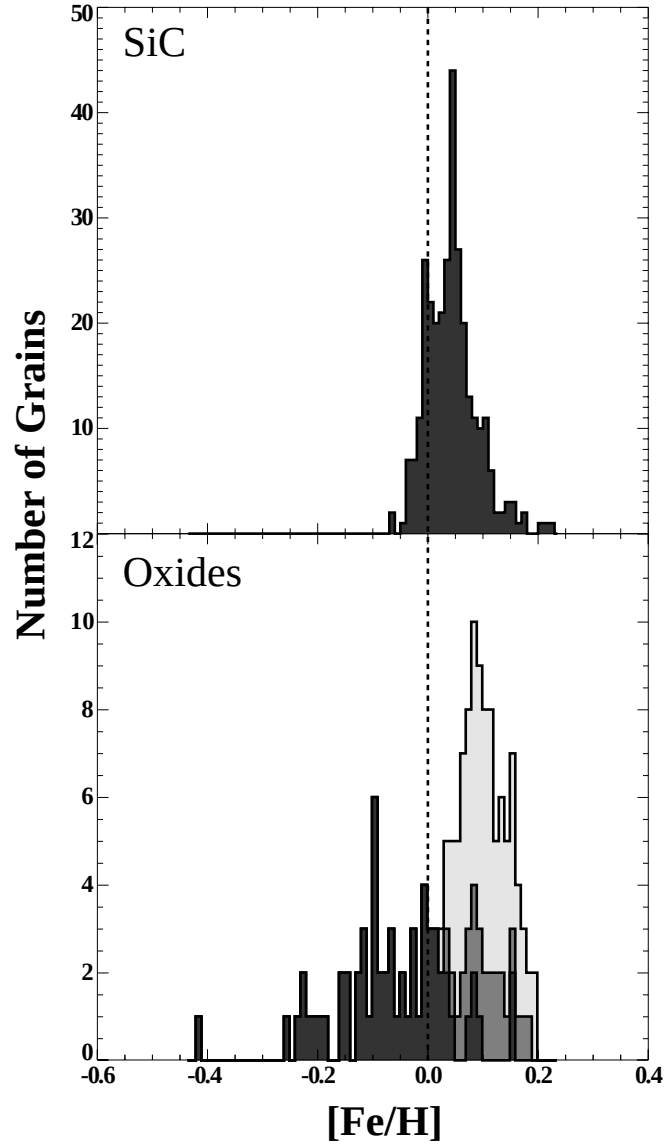


FIG. 3.—Histograms of the metallicities of the mainstream SiC grains (Fig. 1) and group 1 and 3 presolar $Al_2O_3$ grains (Fig. 2). We use the usual logarithmic Fe abundance for metallicity: $[Fe/H] = \log (Fe/H) - \log (Fe/H)_\odot$. The SiC metallicities were determined from the normalized TC96 GCE calculation ($[Fe/H] = \delta^{29}Si/962$, Table 4). The $Al_2O_3$ metallicities were inferred from the TWW95 model and the dredge-up calculations of Boothroyd & Sackmann (1999). The darkest gray histogram indicates the observed grains, whereas the lighter areas indicate estimates for the ~25% (*medium gray*) to 50% (*lightest gray*) of grains that are missed by the ion mapping technique employed to find most of the grains. That there is a difference in metallicity distributions is surprising since both come from the same stellar types. The apparently lower metallicity of the $Al_2O_3$ grains suggests they might have originated in stars of systematically lower mass and, therefore, older ages. More problematic is the observation that most SiC grains, and possibly most $Al_2O_3$ grains, apparently came from higher than solar-metallicity stars, yet the grains' parent stars must have formed hundreds of millions to billions of years before the solar system.

## 3. SiC ISOLATION AND ISOTOPIC ANALYSIS

We report the Si and Ti isotopic compositions of SiC grains isolated from the Murchison meteorite. The grains were isolated from the meteorite using techniques that are

similar to those established by Tang et al. (1988) and Amari, Lewis, & Anders (1994). A 5 g sample of the Murchison meteorite was treated several times with 6 M HCl at 100°C in a sealed Teflon bomb. This destroys most metal, sulfides, and carbonates and attacks many of the silicates. Once most reaction with the HCl had ceased, the sample was given alternating treatments of 9 M HF–1 M HCl and 6 M HCl, again at 100°C in the sealed Teflon bomb, to destroy the remaining silicates. After every step, the solution was taken off and centrifuged for 10 hr at $2000 \times g$. Any material that settled out was returned to the bomb along with fresh acid. Once all visible reaction had ceased, elemental S was extracted using $CS_2$ and this was followed by final treatments with 9 M HF–1 M HCl and 6 M HCl. The sample was then treated with 0.5 N $KCr_2O_7$–1 M $H_2SO_4$ at 80°C, after which three washes with 0.1 M $NH_3$ extracted all presolar nanodiamond from the residue as a colloidal suspension. The noncolloidal residue was separated into two density fractions ($<2.5$ g cc$^{-1}$ and $>2.5$ g cc$^{-1}$) and the more than 2.5 g cc$^{-1}$ fraction was subsequently treated with concentrated perchloric acid at 200°C to remove minerals such as $FeCr_2O_3$ and graphite. Finally, the remaining sample after the perchloric treatment was separated by centrifugation into several size fractions based on settling times in a 50:50 mix of isopropanol and water. The nominally greater than 1.5 $\mu$m size fraction was analyzed here.

The SiC grains were analyzed for their Si and Ti isotopic compositions with the Carnegie 6f ion microprobe using a focussed 12.5 kV $O^-$ primary beam, a 10 kV secondary accelerating voltage with a 50 eV energy window, and O flooding to increase secondary ion yields. Synthetic SiC and TiC grains were used as standards for calibration of the instrumental mass fractionation. The mass resolution, $\Delta M/M$, used for the measurements was $\sim$3800. At this resolution, contributions from all isobaric interferences are negligible except for that from $^{50}$Cr to the measurement of $^{50}$Ti. To monitor this potential interference, $^{52}$Cr was measured and the $^{50}$Cr contribution to $^{50}$Ti was subtracted assuming terrestrial Cr isotope ratios. Most of the measured Cr probably came from the use of $KCr_2O_7$ during the dissolution and destruction of solar system–produced $FeCr_2O_3$ in the final treatment step.

A total of 48 SiC grains were analyzed, but we only present and discuss the data for the 20 grains with the smallest analytical uncertainties in their Ti isotopic compositions. These data are given in Table 2.

## 4. Si AND Ti ISOTOPES IN SiC AND THE GALAXY

### 4.1. *How Typical Is the Solar Composition?*

Based on an extensive survey of the elemental compositions, including Si and Ti, of main-sequence disk stars, Edvardsson et al. (1993) concluded that the Sun is "a quite typical star for its metallicity, age and galactic orbit." On this basis, it seems likely that the solar Si and Ti isotopic compositions are also fairly typical. This is supported by the most recent measurement of the Si isotopic compositions of the Galactic cosmic-ray sources, which are within error (50%) of solar (Webber et al. 1990). Determinations of the $^{30}$Si/$^{29}$Si ratios of molecular clouds are within error (15%) of solar (Wolff 1980), despite the fact that the clouds' positions ranged from 0 to 10 kpc from the Galactic center. Greater than solar $^{29,30}$Si/$^{28}$Si ratios reported by Wolff (1980) for these molecular clouds are probably the result of saturation of the $^{28}$SiO spectra (Penzias 1981a). The measured Si isotopic compositions of giant and supergiant stars are, with some exceptions, within error (10%–50%) of solar (Olofsson et al. 1982; Cernicharo et al. 1986; Kahane et al. 1988; Ukita & Kaifu 1988; Wannier et al. 1991; Tsuji et al. 1994). The Ti isotopic ratios of cosmic rays and molecular clouds have not been measured. However, Clegg, Lambert, & Bell (1979) found the Ti isotopic compositions of two late-type dwarf stars and several MS and S giant stars to be within error (25% for the dwarfs and 50% for the giants) of solar.

TABLE 2

ISOTOPIC COMPOSITIONS OF MURCHISON SiC GRAINS

| Grain | $\delta^{29}$Si[a] (permil) | $\delta^{30}$Si (permil) | $\delta^{46}$Ti (permil) | $\delta^{47}$Ti (permil) | $\delta^{49}$Ti (permil) | $\delta^{50}$Ti (permil) |
|---|---|---|---|---|---|---|
| M3-1 ..... | 43 ± 16 | 60 ± 17 | −12 ± 33 | −34 ± 19 | 127 ± 19 | n.m.[b] |
| M3-9 ..... | 80 ± 4 | 66 ± 5 | 113 ± 16 | 44 ± 9 | 118 ± 10 | 203 ± 29 |
| M3-11..... | −29 ± 4 | 5 ± 5 | −15 ± 25 | −12 ± 11 | 41 ± 15 | −15 ± 23 |
| M3-16..... | 102 ± 4 | 87 ± 5 | 114 ± 17 | 45 ± 10 | 13 ± 9 | 241 ± 12 |
| M3-22..... | −46 ± 7 | −26 ± 8 | −73 ± 21 | −40 ± 21 | −67 ± 20 | −132 ± 36 |
| M3-29..... | 18 ± 4 | 29 ± 6 | 16 ± 13 | 4 ± 12 | 13 ± 11 | 91 ± 30 |
| M3-33..... | 12 ± 4 | 19 ± 6 | 6 ± 13 | 6 ± 11 | 20 ± 11 | 54 ± 28 |
| M3-39..... | 19 ± 4 | 35 ± 5 | 77 ± 50 | 36 ± 22 | 29 ± 20 | 223 ± 65 |
| M3-40..... | 19 ± 4 | 25 ± 5 | −14 ± 20 | −25 ± 14 | 2 ± 14 | 101 ± 42 |
| M3-41..... | 34 ± 5 | 45 ± 6 | −1 ± 14 | −7 ± 10 | 10 ± 9 | 58 ± 32 |
| M3-44..... | 14 ± 5 | 24 ± 7 | 0 ± 13 | −18 ± 9 | −11 ± 8 | 23 ± 11 |
| M5-4 ..... | −9 ± 6 | 13 ± 6 | −16 ± 11 | −11 ± 8 | 18 ± 7 | 21 ± 10 |
| M5-6 ..... | 60 ± 3 | 56 ± 4 | 48 ± 20 | 9 ± 18 | 53 ± 18 | 99 ± 30 |
| M5-7 ..... | −41 ± 7 | 8 ± 9 | −124 ± 42 | −67 ± 51 | −59 ± 45 | n.m. |
| M5-9 ..... | 22 ± 3 | 34 ± 5 | −48 ± 11 | −15 ± 10 | 34 ± 11 | 143 ± 24 |
| M5-12..... | 9 ± 4 | 18 ± 7 | −31 ± 18 | −11 ± 14 | 14 ± 13 | 46 ± 25 |
| M5-13..... | 15 ± 6 | 34 ± 6 | −15 ± 20 | −13 ± 20 | −1 ± 21 | 22 ± 21 |
| M5-15..... | 12 ± 10 | 26 ± 9 | −16 ± 17 | −25 ± 17 | −5 ± 18 | 12 ± 30 |
| M5-16..... | 17 ± 3 | 25 ± 4 | −15 ± 8 | −13 ± 5 | 13 ± 6 | 45 ± 9 |
| M5-17..... | 42 ± 5 | 38 ± 6 | −8 ± 20 | 2 ± 21 | 13 ± 17 | 101 ± 26 |

[a] $\delta^i$Si/$^{28}$Si = [($^i$Si/$^{28}$Si)/($^i$Si/$^{28}$Si)$_\odot$ − 1]1000; normalization isotope for Ti is $^{48}$Ti.

[b] n.m. means not measured.

The astronomical data are consistent with a GCE path for the Si isotopes that passes within a few tens of percent (several 100‰) of the solar composition. However, the errors are such that the suggestion by Clayton & Timmes (1997) that the true GCE line for Si isotopes might be displaced to the left of solar in Figure 1 by up to several 100‰ cannot be completely ruled out. As discussed above, such a large difference between the GCE trend and the mainstream SiC trend would require a large He-shell contribution to the Si isotopes in SiC grains. However, the size of this He-shell contribution appears inconsistent with the C isotopic compositions of the grains.

The $^{12}C/^{13}C$ ratios of almost all mainstream SiC grains are less than 80, and most lie in the range 40–60. The C isotopic composition of a C star is a function of (1) the $^{12}C$ abundance and $^{12}C/^{13}C$ ratio in the envelope at the beginning of the AGB, and (2) the amount of $^{12}C$ dredged up during the AGB. The dashed lines in Figure 4 show the evolution of envelope compositions of solar-metallicity stars as increasing amounts of He-shell material (Table 3) are mixed into them, assuming no cool-bottom processing has occurred on the RGB. The solid squares indicate the point at which the envelope C/O ratio of the model stars becomes greater than one. Without CBP, AGB stars do not become C stars until their $^{12}C/^{13}C$ ratios have exceeded those of most mainstream SiC grains. The assumed $^{12}C$ mass fraction in the He shell in Figure 4 is 0.2, but the $^{12}C/^{13}C$ ratio at which a star becomes a C star is independent of this value. In fact, very high metallicity AGB stars ([Fe/H] $\approx$ 0.4) could become C stars with ratios near 40. However, such a metallicity is very high even for stars forming at the present time and seems unreasonably high given that the grains' parent stars must have formed hundreds of millions to billions of years before the solar system. As we will see, it is also much higher than metallicity estimates from the Si and Ti isotopic compositions of the mainstream grains.

The solid lines in Figure 4 indicate the evolution of the AGB envelope compositions when cool-bottom processing on the RGB is included (Boothroyd & Sackmann 1999); the solid circles indicate the point at which C/O > 1. CBP on the RGB, which operates in stars $\lesssim 2\ M_\odot$, lowers the total C content and $^{12}C/^{13}C$ ratio in the envelope. Table 3 lists the calculated envelope compositions of 1, 1.5, and 2 $M_\odot$ solar-metallicity stars at the start of the AGB, assuming CBP has taken place during the RGB phase. Also given is the calculated composition of the He shell taken from the works of Boothroyd & Sackmann (1988) and Gallino et al. (1994). When CBP is taken into account, all stars $\lesssim 2\ M_\odot$

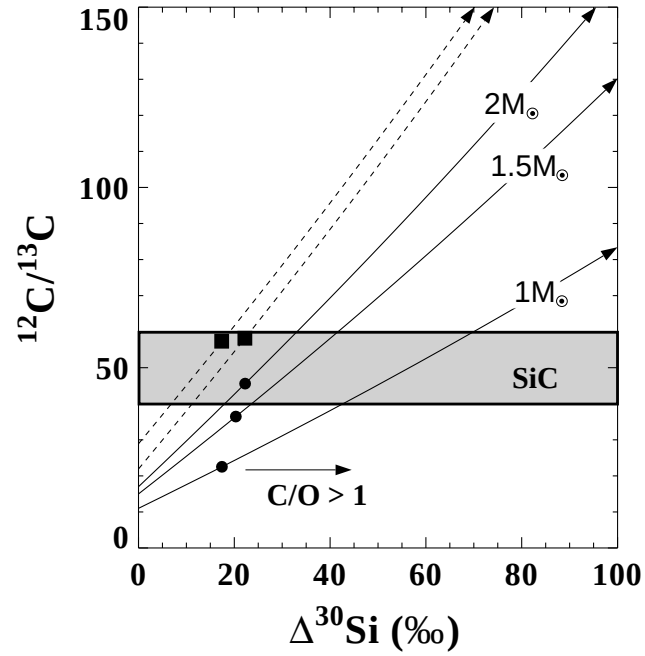


FIG. 4.—Compositional evolution of AGB star envelopes as He-shell material is progressively mixed in to them (Table 3). $\Delta^{30}Si$ is the permil change in the $^{30}Si/^{28}Si$ ratio, relative to the initial envelope composition. The $^{12}C$ mass fraction in the He-shell material is assumed to be 0.2. The gray region indicates the range of $^{12}C/^{13}C$ ratios for most mainstream SiC grains. Two sets of lines are shown. The dashed lines indicate 1 and 2 $M_\odot$ stars that do not experience CBP on the RGB (*lower and upper curves, respectively*). The solid squares mark the point at which they become C stars (C/O > 1). The solid lines are for 1, 1.5, and 2 $M_\odot$ stars that do experience CBP on the RGB; the solid circles mark where these stars become C stars. It seems CBP is required to explain the $^{12}C/^{13}C$ ratios of mainstream SiC grains. Also, since most C stars are thought to be $\gtrsim 1.5\ M_\odot$, it seems the $\delta^{30}Si$ compositions of the SiC parent stars cannot have been modified by third dredge-up by more than $\sim$40‰.

TABLE 3

COMPOSITIONS OF THE SUN, EARLY-AGB ENVELOPES OF THREE SOLAR-METALLICITY STARS, AND AN AGB STAR HE SHELL

| Isotope | Solar | 1 $M_\odot$ | 1.5 $M_\odot$ | 2 $M_\odot$ | He Shell |
|---|---|---|---|---|---|
| $^{12}C$[a,b] | $4.3 \times 10^{-3}$ | $3.5 \times 10^{-3}$ | $3.0 \times 10^{-3}$ | $2.8 \times 10^{-3}$ | 0.20–0.25 |
| $^{12}C/^{13}C$ | 90 | 11 | 15 | 17 | $\infty$ |
| $^{16}O$ | $9.60 \times 10^{-3}$ | $9.58 \times 10^{-3}$ | $9.60 \times 10^{-3}$ | $9.60 \times 10^{-3}$ | 0.02 |
| $^{28}Si$[c] | $6.53 \times 10^{-4}$ | $6.53 \times 10^{-4}$ | $6.53 \times 10^{-4}$ | $6.53 \times 10^{-4}$ | $6.16 \times 10^{-4}$ |
| $\delta^{29}Si/^{28}Si$ | 0 | 0 | 0 | 0 | 429 |
| $\delta^{30}Si/^{28}Si$ | 0 | 0 | 0 | 0 | 913 |
| $^{48}Ti$ | $2.15 \times 10^{-6}$ | $2.15 \times 10^{-6}$ | $2.15 \times 10^{-6}$ | $2.15 \times 10^{-6}$ | $1.09 \times 10^{-6}$ |
| $\delta^{46}Ti/^{48}Ti$ | 0 | 0 | 0 | 0 | 3760 |
| $\delta^{47}Ti/^{48}Ti$ | 0 | 0 | 0 | 0 | 846 |
| $\delta^{49}Ti/^{48}Ti$ | 0 | 0 | 0 | 0 | 7150 |
| $\delta^{50}Ti/^{48}Ti$ | 0 | 0 | 0 | 0 | 21800 |

[a] Abundances are expressed as weight fractions, $\delta$ values in permil (‰).

[b] Envelope C and O abundances are from Boothroyd & Sackmann 1999 and include the effects of cool-bottom processing on the red giant branch. He-shell C and O abundances are from Boothroyd & Sackmann 1988.

[c] Si and Ti abundances and isotopic compositions are from Gallino et al. 1994.

become C stars with $^{12}C/^{13}C$ ratios of 40 or less. It seems that CBP is required to explain the mainstream grains' $^{12}C/^{13}C$ ratios. The 1 $M_\odot$ star has the highest $^{12}C$ envelope abundance and lowest $^{12}C/^{13}C$ ratio, and therefore requires the largest He-shell contribution to produce a typical $^{12}C/^{13}C$ ratio for a mainstream grain. Assuming a 1 $M_\odot$ star with a He-shell $^{12}C$ abundance of 0.2, a $^{12}C/^{13}C$ ratio of 80 requires a He-shell fraction in the envelope of $\sim 0.11$. This would result in a $\sim 100‰$ increase in $\delta^{30}Si$. However, most C stars are thought to have masses that are $\gtrsim 1.5\ M_\odot$ and most mainstream grains have compositions in the range 40–60. To produce $^{12}C/^{13}C$ ratios of 40–60 with a He-shell $^{12}C$ abundance of 0.2 requires He-shell fractions of 0.03–0.05 in a 1.5 $M_\odot$ star and 0.02–0.04 in a 2 $M_\odot$ star. Thus, the C isotopic ratios of most mainstream SiC grains limit the amount of dredged-up material to only a few percent and a change in $\delta^{30}Si$ of a few tens of permil.

The Si and Ti isotopic compositions of presolar SiC grains can be measured with much higher precision than the astronomical observations described above, generally of the order of 1%–5% or better (see Table 2). This enables a more detailed examination of the relationship between the solar composition and the mean GCE paths of the Si and Ti isotopes. Two extreme cases can be envisaged that would produce a range of Si and Ti isotopic compositions in the grains. In one, the isotopic compositions are dominated by the initial compositions of their parent stars. This being the case and if the GCE paths pass close to solar, then in plots of the grains' Si and Ti isotopic compositions the data should form trends that also pass close to solar. If, on the other hand, they are primarily influenced by the addition of He-shell material to stellar envelopes with a limited compositional range, the grains should fall on a mixing line between the He-shell and envelope compositions. We have already seen (Fig. 1) that the Si isotopes of the mainstream SiC grains form a trend that is distinct from that expected for simple mixing of He-shell material into the envelopes of stars with a limited compositional range. The Si and Ti isotopic data for our SiC grains (Table 2) are shown in Figure 5, along with data for 30 grains from the literature (Ireland, Zinner, & Amari 1991; Hoppe et al. 1994). In Figure 5*b*, $\delta^{29}Si$ clearly correlates with $\delta^{46}Ti$, and the direction of the $\delta^{29}Si$-$\delta^{46}Ti$ trend is quite distinct from that expected for mixing between a single or restricted envelope composition and He-shell material. Also, the solar composition falls within the range of the grain data. The correlations between the other Si and Ti isotopes are not always as strong (Fig. 5), but in all cases they are consistent with: (1) the initial envelope compositions dominate the isotopes of the two elements in the SiC grains, and (2) the solar Si and Ti isotopic compositions lie within 1%–2% of the trends in the grain data.

### 4.2. *Grain Data Compared to GCE Models*

Above it was established that the solar composition lies close to the overall GCE trends for Si and Ti isotopes. That is, the Sun is fairly typical for these elements for its age and Galactocentric radius. This justifies, at least for these elements, the normalization scheme for GCE models. It also enables more quantitative estimates of the He-shell contributions to the Si and Ti isotopes of the mainstream SiC grains. The normalized TWW95 and TC96 results for Si and Ti are overlain on the grain data in Figure 5 (*dashed lines*). Also shown in Figure 5 are mixing lines connecting the solar composition with the calculated solar-metallicity He-shell composition (Table 3). Most of the SiC grain data fall on the He-shell side of the model GCE trends, as would be expected if the grain data are simple mixtures of initial envelope material, with variable metallicities, and He-shell material. In the original TWW95 results, the Ti isotopes give among the poorest fits to the solar composition. The rather remarkable consistency of the normalized results with the grain data would seem to validate the normalization scheme.

Ti has five isotopes, and the He shell of an AGB star is calculated to have large but variable enrichments in the isotopes $^{46,47,49,50}Ti$, relative to the most abundant isotope, $^{48}Ti$, and solar (Table 3). Thus, the isotopic composition of Ti is sensitive to the addition of even small amounts of He-shell material. Given that the grain data are consistent with their being mixtures of He-shell and initial envelope material, and are not expected to be influenced by any other process, we have estimated the He-shell content and stellar metallicity for each grain. A $\chi^2$ fit was performed on the Ti isotopic compositions of each of the grains. The fit assumed that the Ti isotopic composition of each SiC grain is a mixture of an initial envelope composition given by the normalized TWW95 and TC96 models and a He-shell isotopic composition given by the calculations of Gallino et al. (1994) for a solar-metallicity AGB star. The change in the relative abundances of $^{28}Si$ and $^{48}Ti$ resulting from nucleosynthesis in the He shell was assumed to always be that for the solar composition star (Table 3). Gallino et al. (1994) calculated He-shell compositions for nonsolar-metallicity stars but assumed a rather different GCE for the Si and Ti isotopes than that calculated by TWW95 and TC96. Although the initial stellar composition will influence to some degree the final He-shell abundances, we have chosen to only use the solar composition He-shell results because solar is the only composition that the two studies share.

The results of the fit suggest that the proportion of He-shell $^{48}Ti$ is less than 1% in most of the grains. Based on the He-shell composition in Table 3 this would imply that the proportion of He-shell material in the envelopes of the grains' parent stars was only about 1%. As discussed above, this is less than seems to be required by the grains' $^{12}C/^{13}C$ ratios (Fig. 4). Also, for SiC to condense, the atomic C/O must be at least one in the stellar envelopes, but, even under the most favorable assumptions (1 $M_\odot$ and a $^{12}C$ weight fraction of 0.25 in the He shell), the C/O ratios estimated from the fits are less than one. Clearly, the fit has underestimated the amount of He-shell material that was dredged up into the envelopes of the grains' parent stars. Barring significant errors in the stellar evolution models, this implies that the true GCE paths must be displaced somewhat from those calculated by TWW95 and TC96 and normalized to go through solar.

### 4.3. *Best Estimates of the* Si *and* Ti *GCE Paths*

Apart from underestimating the fraction of dredged-up He-shell material, mixing of the normalized GCE models and He-shell material cannot explain several other features of the grain data. The steeper slope and nonsolar intercept of the mainstream Si isotope trend is the most obvious discrepancy. Removal of the He-shell Si from the grain compositions using the previous fit results does not significantly alter the slope of the grain trend and only shifts the trend by about 10‰ toward solar. In addition, many of the

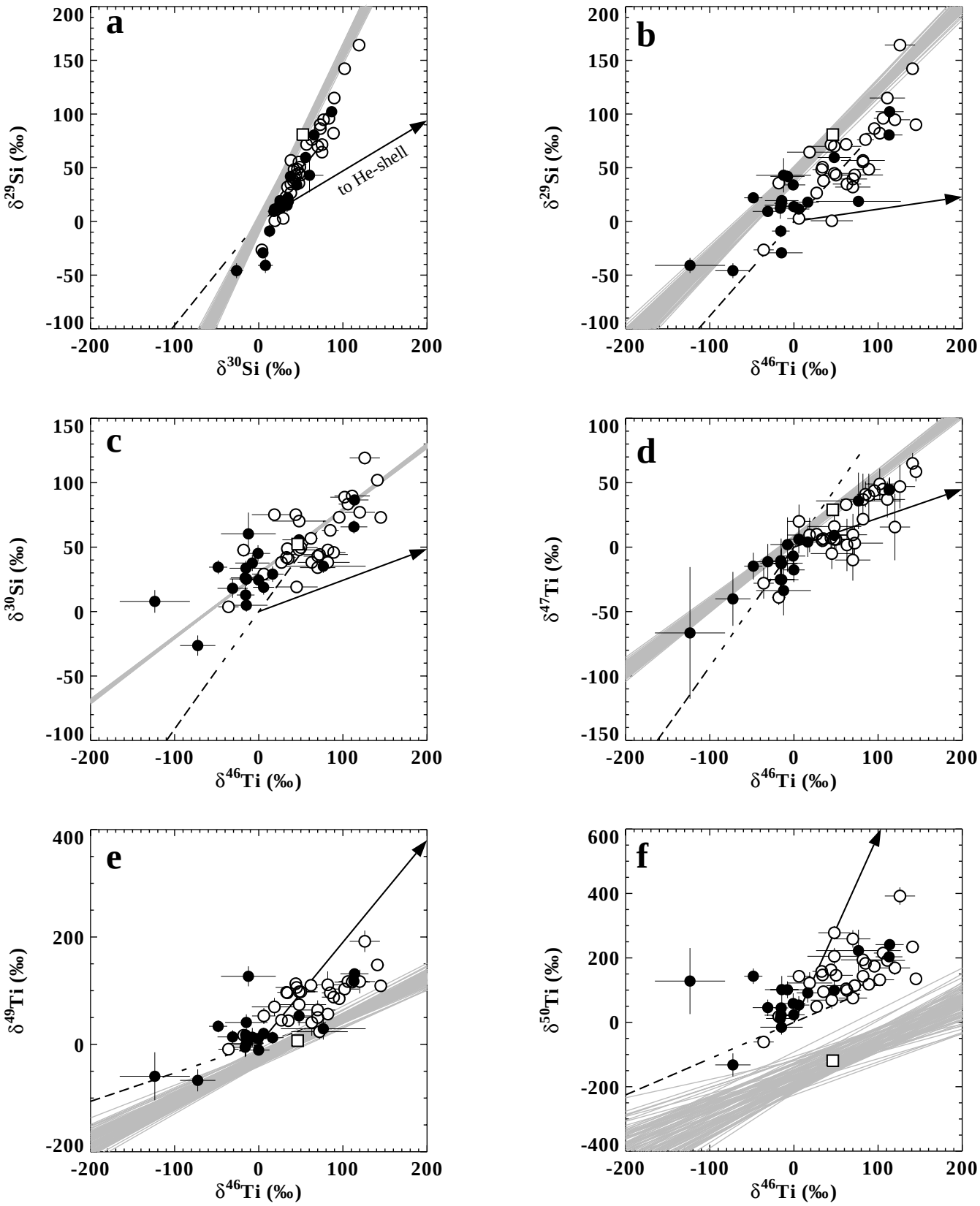


FIG. 5.—Si and Ti isotopic compositions of mainstream SiC grains. Filled circles are from this work; open symbols are from Ireland et al. (1991) and Hoppe et al. (1994). Also shown are the solar normalized TWW95 and/or TC96 GCE paths (*dashed lines*), mixing lines between solar and the He shell of a solar-metallicity star (Table 3, *solid arrows*), and the range of GCE paths found in the $\chi^2$ fits to the grain data (§ 4.3, *gray lines*). The open squares show the average compositions of the interstellar medium at solar metallicity, from the $\chi^2$ fits. In general, the positions of the paths on these plots are well constrained, although compositions at solar metallicity are more variable (Table 4). The least well-constrained paths involve $\delta^{50}$Ti; this isotope is very sensitive to the mass fraction of He-shell material added to the stellar envelopes and thus is most sensitive to uncertainties in the AGB star models. The best-fit GCE paths for most isotopes are remarkably close to those of the TWW95 and TC96 models. The exceptions, $^{30}$Si and $^{47}$Ti, indicate that the supernova yields used by TWW95 and TC96 are incorrect for these isotopes.

data points in Figure 5 lie on the opposite side of the GCE trends to that of the He-shell composition and thus cannot be explained through mixing of these two components. Finally, the model GCE lines in Figure 5 all represent the same metallicity range ([Fe/H] $\approx -0.14$ to 0.08), the upper metallicity limit being the model's present-day value. The range of Ti isotopic compositions exhibited by the SiC grains can largely be explained by the mixing of He-shell material and the envelope model. Yet, there are numerous grains with $\delta^{29,30}$Si compositions that plot far beyond the tip of the model Si isotope line (Fig. 5*a*). Perhaps the Si isotopes evolved faster than has been calculated. Alternatively, the solar Si isotopic composition may be somewhat atypical, and the average composition at [Fe/H] = 0 to which the GCE model should have been normalized is enriched in $^{29}$Si and $^{30}$Si, compared to solar.

In an attempt to resolve some of these discrepancies, we have conducted a second $\chi^2$ fit to the mainstream SiC grain data. Again, the data are assumed to be mixtures of He shell and initial envelope material, the He-shell Si and Ti isotopic compositions are those given in Table 3, the initial $^{28}$Si and $^{48}$Ti abundances were varied as a function of metallicity according to the normalized TWW95 and TC96 models, and the fractional changes in the $^{28}$Si and $^{48}$Ti abundances in the He shell are always the same as calculated for a solar composition star. However, in this fit, the GCE paths of the Si and Ti isotope ratios, expressed as delta values, are treated as unknowns and are not constrained to go through solar. In the normalized GCE models, the Si and Ti isotope delta values evolve essentially linearly with [Fe/H] over the metallicity range considered here ([Fe/H] $\gtrsim -0.2$), and they are assumed to do so here: $\delta = I + S$[Fe/H], where $I$ is the average composition of the ISM when [Fe/H] = 0 and $S$ is given in ‰ dex$^{-1}$. The free parameters of the fit were the metallicity and He-shell fraction of each grain, and the slopes and intercepts of the GCE paths for each of the isotope ratios.

To gauge the topography of the $\chi^2$ surface, we conducted a survey of 100 fits, each starting from initial conditions that were chosen randomly from a broad range of slopes and intercepts (slopes from 0‰ to 2000‰ dex$^{-1}$ and intercepts from $-200$‰ to $+200$‰). It appears that the $\chi^2$ surface is broad and flat in the region of the solution. As a result, progress becomes very slow near the solution and no unique solution was found. This is at least in part because in the fit the He-shell composition is not metallicity dependent and, therefore, the metallicity dependence of the solution is weak. It may also reflect the fact that GCE is a stochastic process and no two stars (or the grains from them) are likely to have had the same initial compositions even if they had the same metallicities. The range of results from the survey was used to constrain the range of the randomly chosen initial conditions for a second set of more accurate fits (more iterations). Again, every fit reached a preset maximum number of iterations before it converged on a unique solution. Nevertheless, the ranges of results are fairly narrow, particularly the relative GCE paths of the isotopes that are plotted in Figure 5 (*gray lines*). This fit also predicts C/O ratios in the grains' parent star envelopes that are greater than one. The means and standard deviations of the slopes and intercepts from the second 100 fits are summarized in Table 4.

As can be seen from Figure 5, the best-fit GCE paths are generally subparallel to those of the GCE models and, except for $\delta^{50}$Ti, are quite well constrained on three-isotope plots. For example, the 100 fits give an average slope of 1.60 for the GCE Si isotope trend, with a standard deviation of 0.05. The larger range in solutions for $\delta^{50}$Ti reflects the fact that it is the most sensitive ratio to the addition of He-shell material. Furthermore, the measurements of $\delta^{50}$Ti typically have larger errors associated with the correction for $^{50}$Cr. As discussed earlier, the absolute variations of the delta values as a function of metallicity are less well constrained than the relative variations. This is evidenced by the large uncertainties (standard deviations in the 100 fits) in the slopes and intercepts of the GCE paths (Table 4).

TABLE 4

GCE Paths of Si and Ti Isotopic Ratios[a]

| Isotopic Ratio | Model Slope[c] (‰ dex$^{-1}$) | $\chi^2$ Fit[b] Intercept (‰) | $\chi^2$ Fit[b] Slope (‰ dex$^{-1}$) |
|---|---|---|---|
| $\delta^{29}$Si/$^{28}$Si ..... | 962 | 81 ± 11 | 934 ± 104 |
| $\delta^{30}$Si/$^{28}$Si ..... | 999 | 52 ± 6 | 585 ± 54 |
| $\delta^{46}$Ti/$^{48}$Ti..... | 1097 | 46 ± 12 | 1180 ± 106 |
| $\delta^{47}$Ti/$^{48}$Ti..... | 1014 | 29 ± 7 | 595 ± 62 |
| $\delta^{49}$Ti/$^{48}$Ti..... | 583 | 7 ± 10 | 894 ± 71 |
| $\delta^{50}$Ti/$^{48}$Ti..... | 1239 | −119 ± 27 | 1347 ± 215 |

[a] Isotopic ratios assumed to evolve linearly with metallicity: $\delta$ = Intercept + Slope[Fe/H].

[b] Fit to SiC data, see § 4.3.

[c] Normalized calculations of Timmes et al. 1995 and Timmes & Clayton 1996. Intercepts are by definition 0 in normalized GCE models.

In Figure 5, the biggest differences between the fitted relative evolution lines and those of the normalized GCE models involve $\delta^{30}$Si (Figs. 5*a* and 5*c*) and $\delta^{47}$Ti (Fig. 5*d*). For instance, in the plot of $\delta^{29}$Si versus $\delta^{30}$Si (Fig. 5*a*), instead of reducing the slope of the GCE line inferred from the mainstream trend so that it is more in line with the TC96 results, the fit suggests that subtraction of the He-shell component steepens it to about 1.6. Thus, it seems that the average GCE path for the Si isotopes indeed has a slope significantly greater than 1 on a three-isotope $\delta$ plot, contrary to the theoretical expectations. This result does not change significantly if the He-shell Si isotopic compositions are allowed to vary as a function of metallicity according to the calculations of Gallino et al. (1994) because the calculated He-shell $\delta^{29}$Si and $\delta^{30}$Si compositions are relatively insensitive to metallicity. However, new, unpublished calculations briefly discussed by Hoppe et al. (1997) indicate that $^{29}$Si and $^{30}$Si are more enriched in the He shell of low-metallicity AGB stars than was calculated by Gallino et al. (1994).

The inferred slopes of the evolutionary paths for $\delta^{29}$Si, $\delta^{46}$Ti, and $\delta^{50}$Ti are comparable to those of the normalized TWW95 and TC96 models (Table 4). In contrast, the slopes of both $\delta^{30}$Si and $\delta^{47}$Ti are significantly lower and that of $\delta^{49}$Ti is higher than those of the normalized models. As discussed above and by Clayton (1988), the ratio of a secondary isotope to a primary one is expected to increase with metallicity during GCE, whereas a primary/primary ratio would be expected to be constant. TC96 showed that current stellar nucleosynthesis calculations yield purely primary $^{28}$Si and purely secondary $^{29}$Si and $^{30}$Si. The good agreement of our fit for $^{29}$Si/$^{28}$Si with the normalized TC96 calculation is consistent with $^{29}$Si being purely secondary

and $^{28}$Si purely primary. However, the lower evolutionary slope of the $^{30}$Si/$^{28}$Si ratio suggests that, in fact, the nucleosynthesis of $^{30}$Si includes a primary component. The shallow slope of $^{47}$Ti/$^{48}$Ti suggests a similar conclusion for the nucleosynthesis of $^{47}$Ti. In other words, the fit results indicate that in the normalized GCE models the abundances of $^{30}$Si and $^{47}$Ti are too low at low metallicity, and that at higher metallicity they increase too rapidly relative to the other isotopes. Similarly, the higher inferred slope for the GCE of $^{49}$Ti/$^{48}$Ti from our fit, compared to the normalized TWW95 calculation, suggests that the abundance of $^{49}$Ti increases too slowly near solar metallicity in the model. That is, $^{49}$Ti is less primary than the models predict.

The discrepancy between the observed slope of the Si isotope GCE trend on a Si three-isotope plot (Fig. 5*a*) and the slope predicted by TC96 is best explained by an overproduction of $^{30}$Si, relative to $^{28}$Si and $^{29}$Si, in the model at metallicities close to solar. Silicon-30 is overproduced by almost a factor of 2 in the original, unnormalized TC96 model, while the $^{29}$Si abundance is only slightly higher than solar. Both $^{29}$Si and $^{30}$Si are mainly produced by hydrostatic Ne burning in Type II supernova progenitors, with a lesser contribution from explosive Ne burning (Table 1). That the solar-metallicity Type II supernova models used by TWW95 and TC96 overproduce $^{30}$Si, relative to $^{28}$Si and $^{29}$Si, is supported by the compositions of the rare supernova-derived SiC grains X and presolar $Si_3N_4$ grains (Amari et al. 1992; Nittler et al. 1995). These grains show an excess of $^{29}$Si relative to $^{30}$Si compared to the supernova models, although from the grains-X data alone it cannot be determined whether the models underproduce $^{29}$Si or overproduce $^{30}$Si. The $\delta^{29}$Si versus $\delta^{30}$Si slope of the SiC X-grain data is $\sim 0.67$ and if one multiplies the gradient of $\delta^{30}$Si versus [Fe/H] in the normalized TC96 model by this factor, the resulting slope in a plot of $\delta^{29}$Si versus $\delta^{30}$Si becomes $\sim 1.5$, not very different from the slope of 1.6 given by our fit.

Titanium-47 is the most underproduced of the Ti isotopes in the original model of TWW95, followed by $^{50}$Ti. The normalization to solar corrects the underproduction to some degree, but still $^{47}$Ti grows in faster in the model at near-solar metallicities than indicated by the grain data. Thus, even the normalized model underproduces $^{47}$Ti relative to the other isotopes at earlier times. Type II supernovae are believed to be the primary sources of $^{47}$Ti (Table 1). On the basis of Ti isotopic data from presolar supernova graphite grains, it has been suggested that $^{47}$Ti production rates are higher in these stars than predicted by supernova models (Amari & Zinner 1997). However, our fit suggests that if this is the case, this effect should be more important in low or intermediate metallicity supernovae than in solar-metallicity ones, in order to explain the shallow slope of the $\delta^{47}$Ti versus [Fe/H] trend near-solar metallicity.

In general, the fitted evolution lines pass close to solar, the exception being $\delta^{50}$Ti. The fitted $\delta^{50}$Ti evolution lines more or less parallel the normalized model results but they are displaced to lower $\delta^{50}$Ti compositions, largely because $^{50}$Ti is so enriched in the calculated *s*-process composition. It is striking how the least $^{50}$Ti enriched grains form a trend that passes through solar. This may simply be coincidence but possibly the calculated $^{50}$Ti enrichment in the He shell has been overestimated. As pointed out by Gallino et al. (1994), the neutron capture cross sections of the Ti isotopes at AGB He-shell temperatures are much less certain than those of the Si isotopes, particularly for neutron-magic $^{50}$Ti. Clearly, a more accurate determination of the $^{50}$Ti neutron capture cross section at He-shell temperatures is essential if the He-shell contributions and Galactic chemical evolution paths are to be determined more accurately from presolar grain isotopic data.

As discussed at the beginning of this section, when comparing the SiC data to the normalized TWW95 and TC96 models, the Si isotopes imply a larger range of metallicities for the grains than do the Ti isotopes. This difference could be explained if, in reality, the Si isotopes evolved faster as a function of metallicity than was calculated by TC96 or, alternatively, if the Sun's Si isotopic composition is somewhat atypical for a [Fe/H] = 0 star. Keeping both the slopes and intercepts of the GCE paths as free parameters in our $\chi^2$ fit allows us to investigate these alternative possibilities. The similar slopes of $\delta^{29}$Si and $\delta^{46}$Ti versus [Fe/H] in both the theoretical model and in the fit (Table 4) would seem to argue against the first explanation. On the other hand, the fit's mean Si isotopic composition is $\delta^{29}$Si = 81‰ and $\delta^{30}$Si = 52‰, suggesting that the Si isotopic composition of the Sun is indeed atypical for a solar-metallicity star. Except for $\delta^{50}$Ti, the isotopic composition of Ti at [Fe/H] = 0 is closer to solar than the isotopic composition of Si. The Si isotopic composition is heavier than the mean of the SiC Si isotope distribution and, if correct, implies that most grains did not come from stars with supersolar metallicities. Figure 6 shows a rescaled inferred metallicity distribution for the SiC parent stars, assuming that [Fe/H] = 0 corresponds to $\delta^{29}$Si $\approx$ 80. This renormalization of the SiC metallicities reduces the difference in metallicity distributions of the presolar SiC and the $Al_2O_3$ parent stars, although the $Al_2O_3$ distribution still extends to lower metallicities (compare Fig. 3).

Finally, as discussed in § 4.1, the C isotopic composition of a C star is a function of its composition at the start of the AGB and the amount of $^{12}$C dredged up on the AGB. Our

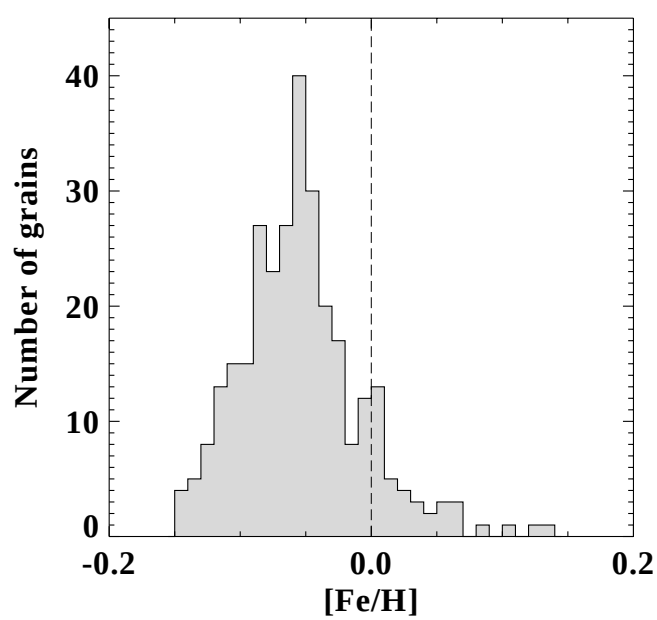


FIG. 6.—Metallicity distribution inferred for parent stars of mainstream SiC grains, assuming that typical stars with solar metallicity ([Fe/H] = 0) are enriched in the heavy Si isotopes, relative to the Sun. Compare with Fig. 3.

fit to the SiC data gives an estimate of the amount of dredge-up that has occurred, which, assuming a $^{12}C$ abundance of 20%–25% by weight (Table 3) in the dredged-up material, gives the amount of $^{12}C$ added to the envelope. The mass of a grain's parent star can then be estimated by finding the mass-dependent early-AGB composition (Boothroyd & Sackmann 1999) that best reproduces the $^{12}C/^{13}C$ ratio of the grain when the dredged-up $^{12}C$ is added to it. Initial results with literature data (we did not determine $^{12}C/^{13}C$ ratios of our SiC grains) suggest that most parent stars were less than $\sim 2\ M_{\odot}$. Without more accurate estimates of the $^{12}C$ abundance in the dredged-up He-shell material it is not possible to pin down the progenitor masses any further.

## 5. O AND Ti ISOTOPES IN $Al_2O_3$ AND THE GALAXY

As with Si, the O isotopic composition of the Galactic cosmic-ray source(s) is close to solar, within $\sim$50% errors (Webber et al. 1996). The same does not appear to be true of the interstellar medium, however. The $^{16}O/^{18}O$ ratio measured in molecular clouds is observed to increase with distance from the Galactic center, and is close to solar at the solar Galactocentric radius of $\sim$8.5 kpc (Wilson & Rood 1994). The measured $^{18}O/^{17}O$ ratio of molecular clouds, on the other hand, is constant throughout the Galaxy, with a value of 3.2, 60% of the solar value (Penzias 1981b; Wilson & Rood 1994). Both the Galactic gradient of $^{18}O/^{16}O$ and the lack of a gradient in $^{18}O/^{17}O$ are predicted by models of GCE (Prantzos, Aubert, & Audouze 1996) and reflect the primary nature of $^{16}O$ and the secondary nature of $^{17}O$ and $^{18}O$. However, unless the molecular cloud observations are seriously in error, the large discrepancy between the molecular cloud $^{18}O/^{17}O$ ratio and the solar value suggests that the O isotopic composition of the Sun is not representative of the average GCE. Detailed studies indicate that the problem lies with $^{18}O$; the Sun might have a 60% enrichment in this isotope, relative to the average interstellar medium at the time it was formed (Prantzos et al. 1996).

Two possible GCE O isotopic trends are shown in Figure 2 along with the presolar $Al_2O_3$ data. The trend passing through solar is the normalized TWW95 calculation and the other is based on the molecular cloud observations. The GCE model of Prantzos et al. (1996) predicts essentially the same trend as the TWW95 model. There is little to distinguish between these trends on the basis of the group 1 and 3 $Al_2O_3$ data. However, models of RGB stars indicate that dredge-up in RGB stars will only move their compositions toward lower $^{16}O/^{17}O$ and higher $^{16}O/^{18}O$ ratios, i.e., to the lower right in Figure 2. The fact that several grains plot to the upper left of the molecular cloud trend thus indicates that the true GCE path lies somewhat above this line. Moreover, one would in fact expect a gap between the GCE path and the grain data, since the $^{16}O/^{17}O$ ratios of those stars that had time to evolve and die before the formation of the solar system ($M > 1\ M_{\odot}$) would all have been decreased by dredge-up. As discussed in § 2, however, the concept of a single, monotonic GCE line is probably not valid, and stochastic effects during Galactic evolution likely lead to a spread in O isotopic compositions at any given time (see also Choi et al. 1998). The grain data suggest that such a GCE band probably extends to higher $^{16}O/^{17}O$ than the group 3 trend, in order to explain the bulk of the data.

Note that extending the TWW95 O isotopic trend to higher metallicities makes it pass through the poorly understood group 4 grains. This suggests that these grains might have formed in stars of very high metallicity (up to [Fe/H] $\sim$ 0.5). Although there are some problems with this suggestion (see Nittler et al. 1997), it is intriguing that the abundance of group 4 grains ($\lesssim$4%) in the presolar $Al_2O_3$ data set is similar to the abundance of super–metal-rich stars in the Galactic disk (Castro et al. 1997; McWilliam 1997). The origin of these stars is uncertain, but they may either represent extreme local disk GCE or they may have been scattered out of the more metal-rich Galactic bulge.

The metallicities inferred for the presolar $Al_2O_3$ grains' parent stars depend on the assumed GCE trend for O isotopic ratios. If, as discussed above, the Sun is enriched in $^{18}O$, relative to the average GCE, the normalization used to derive Figure 3 (the normalized TWW95 model) is probably incorrect and the metallicity scale for presolar $Al_2O_3$ grains must be modified. Taken at face value, a 60% excess of $^{18}O$ in the Sun would require a shift upward of about 0.2 dex in the [Fe/H] values inferred for the grains and would imply that essentially all of the $Al_2O_3$ grains came from supersolar-metallicity stars. This complicates the comparison of the inferred metallicity distributions of SiC and $Al_2O_3$ grains. In this regard, it would be very useful to check for internal consistency in metallicity estimates from Si, Ti, and O isotopes. A direct check would be possible with presolar silicate grains. Unfortunately, no such grains have yet been identified in meteorites. However, Ti isotopic data have been obtained for a few presolar $Al_2O_3$ grains (Huss, Fahey, & Wasserburg 1995; Strebel et al. 1997; Choi et al. 1998). We consider the four grains with the smallest errors in their Ti isotopic ratios ($\lesssim$6%). Shown in Figure 7 are the metallicities inferred for the parent stars of these

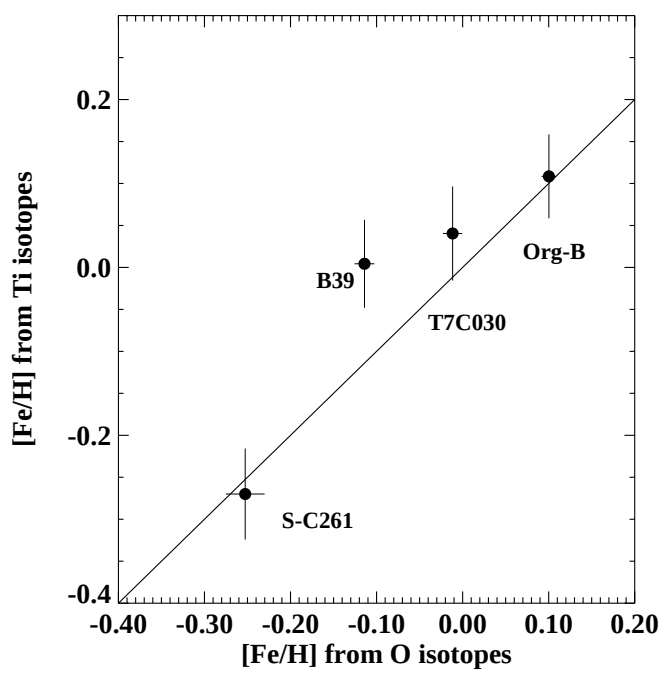


FIG. 7.—Comparison of metallicities inferred for four presolar oxide grains from their O isotopic ratios with those estimated from their Ti isotopic ratios (see text). The solid line indicates agreement between the two methods of estimating [Fe/H] values. That the metallicity estimates are in good agreement suggests that the Sun is not atypically rich in $^{18}O$, relative to the average interstellar medium. Grains Org-B, B39, and S-C261 are from Choi et al. (1998); grain T7C030 is from Strebel et al. (1997).

grains from their O isotopic ratios plotted against those inferred from their Ti isotopic ratios. The O metallicities were determined from the models of Boothroyd & Sackmann (1999), assuming the normalized TWW95 O isotopic evolution. The Ti metallicities were determined from the results of our fit to the SiC data (Table 4) by assuming that the grains' Ti isotopic compositions were purely determined by GCE. The metallicity estimates derived by the two methods are remarkably consistent with each other (the solid line indicates perfect agreement). Given uncertainties in the data and the models, this consistency might be fortuitous, but there certainly does not appear to be a systematic offset of 0.2 dex in the O-derived [Fe/H] values, as suggested by the molecular cloud GCE trend. Clearly, additional isotopic data should help resolve these issues.

## 6. SELF-ENRICHMENT OF THE PRESOLAR CLOUD BY SUPERNOVA EJECTA

Our second fit to the mainstream SiC grain data (§ 4.3) suggests that the typical $\delta^{29}$Si composition of the ISM at about the time the solar system formed was $\sim 81‰$ heavier than solar. If correct, what could have been the cause? One possibility is that the cloud from which the Sun formed was enriched locally by matter expelled from one or more nearby supernova explosions. Self-enrichment of the presolar cloud by supernovae has been invoked to explain the following: (1) an apparent excess in the solar O abundance, relative to young B stars (Gies & Lambert 1992; Kilian 1992; Cunha & Lambert 1994; Kilian, Montenbruck, & Nissen 1994), (2) an apparent excess in solar O relative to the local ISM (Meyer, Jura, & Cardelli 1998), and (3) the high $^{18}$O/$^{17}$O ratio of the Sun, relative to molecular clouds (Penzias 1981b; Wilson & Rood 1994; Prantzos et al. 1996; and § 5). Measurements of dwarf stars also suggest that the Sun has an O excess compared to stars of similar age and metallicity (Gratton 1985; Edvardsson et al. 1993). It has furthermore been suggested that a supernova shock wave triggered the formation of the solar system (Cameron 1962; Foster & Boss 1996) and could also account for some of the short-lived radionuclides present in the early solar system (Cameron & Truran 1977; Olive & Schramm 1982; Foster & Boss 1996).

Addition of enough supernova material to reduce the ISM $\delta^{29}$Si by 81‰ to the solar value would have significant effects on other isotopes. Table 5 shows the mass fraction of supernova Si, Ti, and O that would have to be subtracted from the solar composition to account for the 81‰ deficit in solar $\delta^{29}$Si, for supernovae of a wide range of masses (yields are from Woosley & Weaver 1995). As advocated by TC96, we do not use the observed solar system composition, but rather the composition of the interstellar medium at the time of solar system formation as calculated by TWW95 and TC96. This removes the inconsistency of using stellar yields that do not accurately reproduce the solar composition. Table 5 also shows the isotopic composition of the ISM after subtraction of the supernova component. The supernova yields are mass-dependent but in general the predicted $\delta^{30}$Si values are of the right order compared to the fit results. However, only the 18 $M_\odot$ supernova model predicts a $\delta^{46}$Ti composition that is not in conflict with the fit results.

As can be seen in Table 5, using most supernova models to explain the Si isotopic composition of the fit leads to ISM compositions that are depleted in $^{18}$O relative to solar. Although this would be consistent with the molecular cloud O isotopic measurements, it is problematic for the interpretation of the presolar grain data. In particular, this would have the effect of increasing the metallicities inferred for the $Al_2O_3$ source stars. Using the normalized TWW95 results, one finds that there already may be a large fraction of

TABLE 5

ISM Elemental and Isotopic Composition after Correction for SN Self-Enrichment of the Protosolar Cloud[a]

| Mass ($M_\odot$) | $X_{Si}$ | $\delta^{30}$Si (‰) | $X_{Ti}$ | $\delta^{46}$Ti (‰) | $X_O$ | $\delta^{18}$O (‰) |
|---|---|---|---|---|---|---|
| ISM..... | ... | 52[b] | ... | 46[b] | 0.6[c] | −600[d] |
| 11 ..... | 0.17 | 80 | 0.83 | 3623 | 0.11 | −873 |
| 12 ..... | 0.10 | 90 | 0.13 | −327 | 0.02 | −273 |
| 13 ..... | 0.14 | 59 | 0.32 | 344 | 0.07 | −122 |
| 15 ..... | 0.13 | 70 | 0.17 | −48 | 0.08 | −103 |
| 18 ..... | 0.15 | 44 | 0.10 | 45 | 0.13 | −467 |
| 19 ..... | 0.11 | 90 | 0.05 | −24 | 0.05 | −152 |
| 20 ..... | 0.13 | 88 | 0.06 | −82 | 0.09 | −89 |
| 22 ..... | 0.21 | 67 | 0.14 | −24 | 0.14 | 81 |
| 25 ..... | 0.24 | 76 | 0.14 | −23 | 0.25 | 252 |
| 30 ..... | −0.02 | 58 | −0.01 | −1 | −0.08 | −69 |
| 30 ..... | −0.07 | 74 | −0.08 | −45 | −0.12 | −99 |
| 35 ..... | −0.02 | 42 | −0.02 | −5 | −0.15 | −127 |
| 35 ..... | −0.02 | 57 | −0.01 | 0 | −0.10 | −88 |
| 35 ..... | −0.18 | 66 | −0.21 | −125 | −0.27 | −207 |
| 40 ..... | −0.04 | 30 | −0.06 | −16 | −0.34 | −247 |

[a] For each supernova model, $X_A$ is the mass fraction of element A that must be subtracted from the solar composition to yield an ISM that is enriched in $^{29}$Si by 81‰ (see § 4.3 and Table 4). Supernova yields are from Woosley & Weaver 1995.

[b] Based on fit to SiC data; see Table 4.

[c] Based on the apparent overabundance of solar O, relative to the local ISM (Meyer et al. 1998).

[d] Based on molecular cloud observations; see § 5.

supersolar-metallicity grains (Fig. 3). If the correct reference composition is $^{18}O$ depleted relative to solar, we are faced with the same paradoxes we set out to resolve, namely, (1) that the SiC and $Al_2O_3$ grains give different metallicity distributions, although both will have come from similar stars, and (2) this time the $Al_2O_3$, rather than the SiC, gives metallicities that are greater than solar, yet the stars they came from must have formed hundreds of millions to billions of years before solar system formation. Based on the present supernova models, invoking self-enrichment does not help resolve the paradoxical issues raised by the presolar SiC and $Al_2O_3$ grain data.

The situation gets even more difficult if we try to explain the interstellar and stellar elemental abundance observations in addition to the presolar grain data. For instance, none of the models predict O elemental abundances in the ISM of 0.6 times solar as suggested by the observations. Addition of enough supernova material to produce this difference in O abundances would have consequences for the Si and Ti isotopes that are incompatible with the grain results. Based on these supernova models, it does not seem possible to reconcile the differences between the solar composition and astronomical estimates of stellar and molecular cloud compositions through local enrichment by Type II supernovae. We cannot rule out at this point, however, that improved supernova models, taking into account multidimensional hydrodynamics and updated reaction rates, will change this result.

## 7. CONCLUSIONS

We have attempted to show in this paper that the isotopic compositions of presolar grains in meteorites can provide powerful constraints on the precise manner in which isotopic ratios evolve in the Galaxy. The key point enabling our analysis is that multiple isotopic ratios can be measured with high precision in individual circumstellar grains. Since different isotopes are affected to differing degrees by GCE and stellar nucleosynthesis and mixing, we can deconvolve the GCE and nucleosynthetic components in the isotopic grain data. Whereas previous studies of GCE and presolar grains have *assumed* the theoretical GCE trends to be correct and invoked stellar evolution to explain discrepancies (Gallino et al. 1994; Timmes & Clayton 1996; Clayton & Timmes 1997), we have instead used the data themselves to directly infer the GCE trends. In this way, we can potentially deduce where errors might occur in the theoretical GCE and stellar models.

The major conclusions we draw from this work are as follows:

1. The $^{12}C/^{13}C$ ratios measured in mainstream presolar SiC grains limit the total amount of He-shell material mixed to the surface of the parent AGB stars during third dredge-up to a few percent. This implies that the Si and Ti isotopic ratios of the grains lie close to the Galactic evolutionary trends for these elements and not several tens of percent away, as suggested by Clayton & Timmes (1997). Moreover, the C isotopes in the grains also indicate that most of the parent stars underwent cool-bottom processing prior to becoming AGB stars.

2. The close proximity to the solar composition of the mainstream SiC Si and Ti isotopic ratio trends indicates that the solar isotopic composition of these elements is probably typical of the average interstellar medium to within a few percent. The presolar $Al_2O_3$ grains suggest a similar conclusion for the solar O isotopic composition, but this is not consistent with the O isotopic ratios measured in molecular clouds.

3. We have performed $\chi^2$ fits on the SiC Si and Ti data to infer the GCE trends for these elements. For most of the isotopes the relative evolutionary trends are well constrained and close to the normalized GCE calculations of Timmes et al. (1995) and Timmes & Clayton (1996). Important exceptions are $^{30}Si$ and $^{47}Ti$, for which the models seem to predict too rapid an increase with metallicity at near-solar metallicities (and hence too shallow an increase with metallicity at earlier times) and $^{49}Ti$, for which the models predict too shallow an increase with metallicity. The errors probably lie in the supernova yields used in the GCE calculations and might suggest a primary component for the nucleosynthesis of $^{30}Si$ and $^{47}Ti$. The fitted GCE paths are less well constrained for $^{50}Ti$. This isotope is most sensitive to the details of the AGB nucleosynthesis; our fit suggests that $^{50}Ti$ is overproduced in the AGB model of Gallino et al. (1994).

4. The $\chi^2$ fits also suggest that the Sun is slightly depleted in $^{29}Si$ and $^{30}Si$ (by $\sim 8\%$ and $\sim 5\%$, respectively), relative to the typical solar-metallicity interstellar medium, but has a more typical Ti isotopic composition. If this result is true, the well-known problem of most presolar SiC grains having come from supersolar-metallicity stars is lifted, as is the need to invoke exotic solutions for this problem. Local enrichment (or depletion) of the presolar cloud by one or more supernovae may account for the apparent excess of $^{28}Si$ in the solar system, but it is difficult to account for all the isotopic data with this scenario, at least with current supernova models.

Clearly our results are only as good as the isotopic data and stellar models that have gone into our analysis. Our conclusions would be more robust with a larger and more precise isotopic data set. Moreover, in some recent AGB star models (e.g., Gallino et al. 1998), the neutron capture nucleosynthesis occurs in a fundamentally different fashion than in previous models, such as that of Gallino et al. (1994), which we have used here. A detailed analysis of the effects of the new models on both AGB Si and Ti isotopic ratios is highly desirable to investigate how our conclusions might have to be modified.

The authors would like to thank Erik Hauri and Jianhua Wang for their help and encouragement with the ion probe measurements and Don Clayton and Frank Timmes for sharing results and useful discussions. This work was partially funded by NASA grant NAG5-4328.

REFERENCES


Alexander, C. M. O'D. 1993, Geochim. Cosmochim. Acta, 57, 2869
———. 1997, in AIP Conf. Proc. 402, Astrophysical Implications of the Laboratory Study of Presolar Materials, ed. T. J. Bernatowicz & E. Zinner (New York: AIP), 567
Amari, S., Hoppe, P., Zinner, E., & Lewis, R. S. 1992, ApJ, 394, L43
Amari, S., Lewis, R. S., & Anders, E. 1994, Geochim. Cosmochim. Acta, 58, 459
Amari, S., & Zinner, E. 1997, in AIP Conf. Proc. 402, Astrophysical Implications of the Laboratory Study of Presolar Materials, ed. T. J. Bernatowicz & E. Zinner (New York: AIP), 287
Anders, E., & Zinner, E. 1993, Meteoritics, 28, 490
Begemann, B., Dorschner, J., Henning, T., Mutschke, H., Guertler, J., Koempe, C., & Nass, R. 1997, ApJ, 476, 199
Boothroyd, A. I., & Sackmann, I.-J. 1988, ApJ, 328, 653
———. 1999, ApJ, 510, 232
Boothroyd, A. I., Sackmann, I.-J., & Wasserburg, G. J. 1994, ApJ, 430, L77
Cameron, A. G. W. 1962, Icarus, 1, 13
Cameron, A. G. W., & Truran, J. W. 1977, Icarus, 30, 447
Castro, S., Rich, R. M., Grenon, M., Barbuy, B., & McCarthy, J. K. 1997, AJ, 114, 376
Cernicharo, J., Kahane, C., Gomez-Gonzalez, J., & Guelin, M. 1986, A&A, 167, L9
Choi, B.-G., Huss, G. R., Wasserburg, G. J., & Gallino, R. 1998, Science, 282, 1284
Clayton, D. D. 1988, ApJ, 334, 191
———. 1997, ApJ, 484, L67
Clayton, D. D., & Timmes, F. X. 1997, ApJ, 483, 220
Clegg, R. E. S., Lambert, D. L., & Bell, R. A. 1979, ApJ, 234, 188
Cohen, M. 1984, MNRAS, 206, 137
Cunha, K., & Lambert, D. L. 1994, ApJ, 426, 170
Edvardsson, B., Anderson, J., Gustaffson, B., Lambert, D. L., Nissen, P. E., & Tomkin, J. 1993, A&A, 275, 101
El Eid, M. 1994, A&A, 285, 915
Foster, P. N., & Boss, A. P. 1996, ApJ, 468, 784
Gallino, R., Arlandini, C., Busso, M., Lugaro, M., Travaglio, C., Straniero, O., Chieffi, A., & Limongi, M. 1998, ApJ, 497, 388
Gallino, R., Raiteri, C. M., Busso, M., & Matteucci, F. 1994, ApJ, 430, 858
Gies, D. R., & Lambert, D. L. 1992, ApJ, 387, 673
Gratton, R. G. 1985, A&A, 148, 105
Gratton, R. G., & Sneden, C. 1988, A&A, 204, 193
———. 1991, A&A, 241, 501
Hoppe, P., Amari, S., Zinner, E., Ireland, T., & Lewis, R. S. 1994, ApJ, 430, 870
Hoppe, P., Annen, P., Strebel, R., Eberhardt, P., Gallino, R., Lugaro, M., Amari, S., & Lewis, R. S. 1997, ApJ, 487, L101
Hoppe, P., Strebel, R., Eberhardt, P., Amari, S., & Lewis, R. S. 1996, Geochim. Cosmochim. Acta, 60, 883
Huss, G. R., Fahey, A. J., Gallino, R., & Wasserburg, G. J. 1994, ApJ, 430, L81
Huss, G. R., Fahey, A. J., & Wasserburg, G. J. 1995, Lunar Planet. Sci., 26, 643
Iben, I., Jr. 1991, ApJS, 76, 55
Ireland, T. R., Zinner, E. K., & Amari, S. 1991, ApJ, 376, L53
Kahane, C., Gomez-Gonzalez, J., Cernicharo, J., & Guelin, M. 1988, A&A, 190, 167
Kilian, J. 1992, A&A, 262, 171
Kilian, J., Montenbruck, O., & Nissen, P. E. 1994, A&A, 284, 437
Magain, P. 1989, A&A, 209, 211
Mathews, G. J., Bazan, G., & Cowan, J. J. 1992, ApJ, 391, 719
McWilliam, A. 1997, ARA&A, 35, 503
Merrill, K. M., & Stein, W. A. 1976a, PASP, 88, 285
———. 1976b, PASP, 88, 294
Meyer, D. M., Jura, M., & Cardelli, J. A. 1998, ApJ, 493, 222
Nittler, L. R. 1997, in AIP Conf. Proc. 402, Astrophysical Implications of the Laboratory Study of Presolar Materials, ed. T. J. Bernatowicz & E. Zinner (New York: AIP), 59
Nittler, L. R., Alexander, C. M. O'D., Gao, X., Walker, R. M., & Zinner, E. K. 1994, Nature, 370, 443
———. 1997, ApJ, 483, 475
Nittler, L. R., et al. 1995, ApJ, 453, L25
Olive, K. A., & Schramm, D. N. 1982, ApJ, 257, 276
Olofsson, H., Johansson, L. E. B., Hjalmarson, A., & Nguyen-Quang-Rieu, M. 1982, A&A, 107, 128
Ott, U. 1993, Nature, 364, 25
Penzias, A. A. 1981a, ApJ, 249, 513
———. 1981b, ApJ, 249, 518
Prantzos, N., Aubert, O., & Audouze, J. 1996, A&A, 309, 760
Sloan, G. C., Levan, P. D., & Little-Marenin, I. R. 1996, ApJ, 463, 310
Smith, V. V., & Lambert, D. L. 1990, ApJS, 72, 387
Strebel, R., Hoppe, P., & Eberhardt, P. 1997, Meteoritics and Planet. Sci. 31 (Suppl.), A125
Tang, M., Lewis, R. S., Anders, E., Grady, M. M., Wright, I. P., & Pillinger, C. T. 1988, Geochim. Cosmochim. Acta, 52, 1221
Timmes, F. X., & Clayton, D. D. 1996, ApJ, 472, 723 (TC96)
Timmes, F. X., Woosley, S. E., & Weaver, T. A. 1995, ApJ, 98, 617 (TWW95)
Treffers, R., & Cohen, M. 1974, ApJ, 188, 545
Tsuji, T., Ohnaka, K., Hinkle, K. H., & Ridgway, S. T. 1994, A&A, 289, 469
Ukita, N., & Kaifu, N. 1988, in Proc. IAU Colloq. 108, Atmospheric Diagnostics of Stellar Evolution. Chemical Peculiarity, Mass Loss, and Explosion, ed. K. Nomoto (Berlin: Springer), 51
Wannier, P. G., Andersson, B. G., Olofsson, H., Ukita, N., & Young, K. 1991, ApJ, 380, 593
Wasserburg, G. J., Boothroyd, A. I., & Sackmann, I.-J. 1995a, ApJ, 447, L37
Wasserburg, G. J., Gallino, R., Busso, M., Goswami, J. N., & Raiteri, C. M. 1995b, ApJ, 440, L101
Webber, W. R., Gupta, M., Soutoul, A., & Ferrando, P. 1990, ApJ, 348, 611
Webber, W. R., Lukasiak, A., McDonald, F. B., & Ferrando, P. 1996, ApJ, 457, 435
Wilson, T. L., & Rood, R. T. 1994, ARA&A, 32, 191
Wolff, R. S. 1980, ApJ, 242, 1005
Woosley, S. E., & Weaver, T. A. 1994, ApJ, 423, 371
———. 1995, ApJS, 101, 181
Zinner, E. 1997, in AIP Conf. Proc. 402, Astrophysical Implications of the Laboratory Study of Presolar Materials, ed. T. J. Bernatowicz & E. Zinner (New York: AIP), 3
Zinner, E., Tang, M., & Anders, E. 1989, Geochim. Cosmochim. Acta, 53, 3273